TWO DIMENSIONAL ANALYSIS OF AN E-CORE INDUCTOR

R. Mertens, K. Hameyer and R. Belmans
Katholieke Universiteit Leuven,
Dep. EE (ESAT), Div. ELEN,
Kardinaal Mercierlaan 94,
B-3001 Heverlee,
Belgium

ABSTRACT: One of the aims of a CAD laboratory in electromagnetics is to make students familiar with commercial CAD packages often based on the finite element technique. To avoid an unquestionable believe in computer results, it is useful to compare the classical approaches with the finite element approach. An E-core inductor with its rather simple construction is chosen as a subject of the CAD laboratory and the inductance of a two dimensional approximation is calculated in different ways.

INTRODUCTION

In spite of its rather simple construction, a core of laminated iron and a coil of copper (fig. 1), an E-core inductor has a lot to offer as a subject of a CAD laboratory. In the classical approach, the inductor is seen as a magnetic circuit (flux tube model), or a superposition of flux-*MMF* plots of the different tubes of which the inductor is made. Different approximations either include or exclude the magnetomotive force in the iron parts, the non-linear behaviour of the material, the leakage flux or the fringing effect in the air gap. No effects in the third dimension are taken into account. Because a two dimensional finite element calculation deals inherently with those effects, it is used as reference. The students have to compare and discuss the results and the restrictions of the various methods.

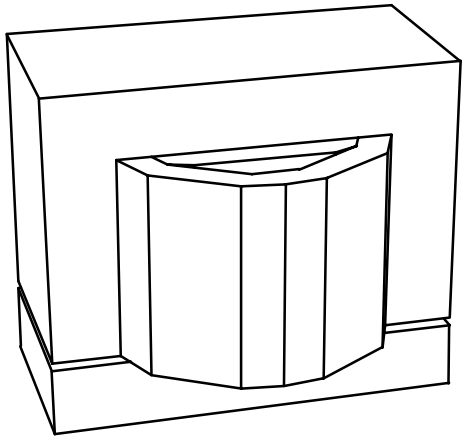

Figure 1: Three dimensional view of the E-core inductor.

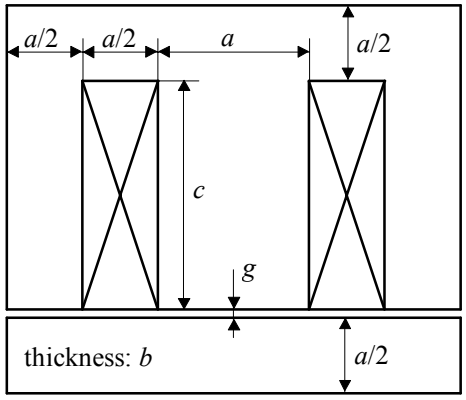

Figure 2: Cross section of the E-core inductor.

Table 1: Rated values and dimensions of the E-core inductor.

L = 150 mH	g = 3.3 mm
I = 10 A	a = 6 cm
N = 288	b = 9 cm
	c = 9 cm

CLASSICAL APPROACH

Magnetic circuit

A magnetic circuit based on Hopkinson's law is a first approach to calculate the inductance L. The magnetic circuit is described by a flux tube model. Reluctances represent the different flux tubes of the model. The inductance is calculated from the total reluctance $\Re_m$.

$$L = \frac{N^2}{\Re_m} \tag{1}$$

where N is the number of turns of the coil.

A first approximation is obtained by only taken the air gap reluctances into account (fig. 3). It can be noted that the magnetic flux through the right or the left leg is half of the flux through the centre leg. This is a parallel connection in terms of a magnetic circuit.

The total reluctance is given by

$$\Re_m = \Re_{m1} + \frac{\Re_{m2}}{2}. \tag{2}$$

$\Re_{m1}$ is the reluctance of the air gap beneath the centre leg and $\Re_{m2}$ is the reluctance of the air gap beneath the right or left leg. The cross-section of the air gap is taken different from the core cross-section to take the fringing effect in the air gap into account. The dimension of the core cross-section is increased with a fraction of the air gap length g at each side. The cross-section S_1 of the air gap beneath the centre leg becomes (neglecting fringing in the third dimension)

$$S_1 = (a + 1...2\,g)\,b\,. \tag{3}$$

$$\Re_{m1} = \frac{g}{\mu_0 (a + 1...2\,g)\,b} \tag{4}$$

$$\Re_{m2} = \frac{g}{\mu_0 \left(\frac{a}{2} + 1...2\,g\right) b} \tag{5}$$

Table 1 and fig. 2 show the dimensions of the inductor used in the CAD laboratory. Table 2 shows the result of the inductance calculation in which the dimension of the core cross-section is increased with the air gap length at each side.

Leakage flux

The reluctance of a rectangular slot with current carrying conductors is calculated to deal with the leakage flux in the E-core inductor, resulting in an improved magnetic circuit of the inductor (fig. 4). The reluctance $\Re_{m3}$ is obtained starting from Ampère's law [4]. This exercise is very useful because it stresses that the general formulae for the reluctance are only valid in case of an uniform field distribution.

$$\Re_{m3} = 3\frac{a/2}{\mu_0\, b\, c} \tag{6}$$

The total reluctance is given by

$$\frac{1}{\Re_m} = \frac{1}{\Re_{m1} + \frac{\Re_{m2}}{2}} + \frac{1}{\frac{\Re_{m3}}{2}}\,. \tag{7}$$

Table 3 shows the result of the inductance calculation based on this improved magnetic circuit.

Fringing effect based on the Carter factor

Two different factors can be used to obtain an improved approximation of the fringing effect in the air gap (fig. 5). The Carter factor, the first one, is defined as the ratio of two air gap lengths, the real length g of the air gap and the equivalent length δ of a smooth air gap (without slots) in which the same magnetic energy is stored.

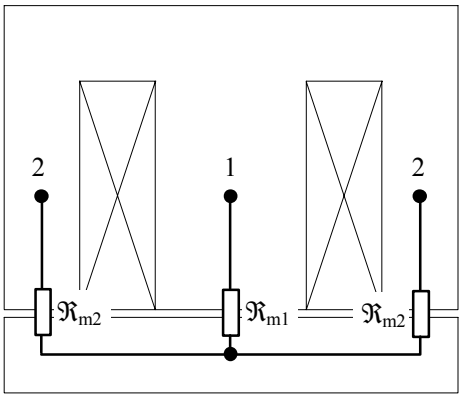

Figure 3: Simplified magnetic circuit of the inductor.

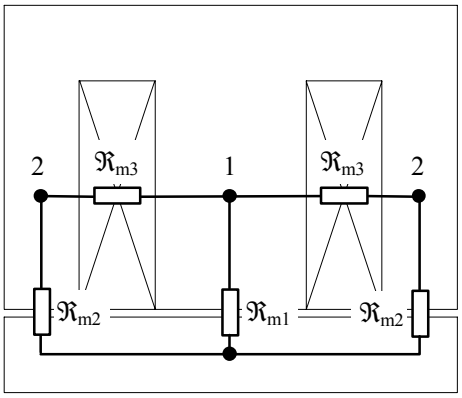

Figure 4: Improved magnetic circuit of the inductor.

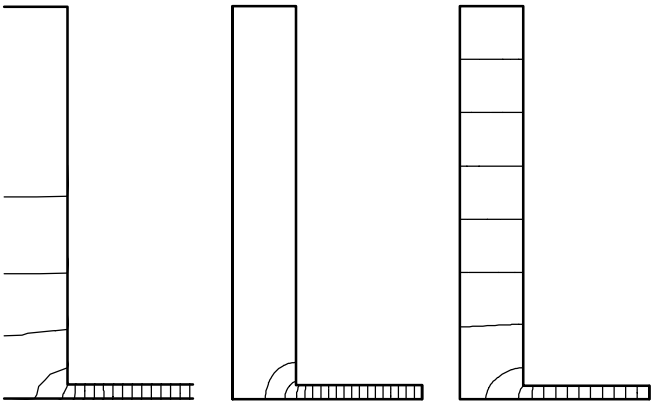

Figure 5: Flux plot of a zone in the air gap of the inductor (a), calculation of the Carter factor (b) and a Carter based factor (c).

Table 2: Inductance calculation based on a simplified magnetic circuit of the inductor.

$\Re_{m1} = 4.381 \cdot 10^5$ H^{-1}	$\Re_m = 8.367 \cdot 10^5$ H^{-1}
$\Re_{m2} = 7.972 \cdot 10^5$ H^{-1}	$L = 0.099$ H

Table 3: Inductance calculation based on an improved magnetic circuit of the inductor.

$\Re_{m1} = 4.381 \cdot 10^5$ H^{-1}	$\Re_m = 7.036 \cdot 10^5$ H^{-1}
$\Re_{m2} = 7.972 \cdot 10^5$ H^{-1}	$L = 0.118$ H
$\Re_{m3} = 8.842 \cdot 10^6$ H^{-1}	

$$k_c = \frac{\delta}{g} \tag{8}$$

The Carter factor is defined as [5, 6]:

$$k_c = \frac{\lambda}{\lambda - \alpha g}, \tag{9}$$

with

$$\alpha = \frac{4}{\pi}\left(\beta \arctan(\beta) - \ln\sqrt{1+\beta^2}\right) \tag{10}$$

$$\beta = \frac{w}{2g} \tag{11}$$

$$\text{slot width } w = \frac{a}{2} \tag{12}$$

$$\text{slot pitch } \lambda = \frac{3a}{2}. \tag{13}$$

The Carter factor can also be calculated by the finite element method (fig. 5b) and is as model very suitable to make the students familiar with the CAD software. Dirichlet boundary conditions are applied at the left and right hand side of the model. The magnetic flux Φ is forced by applying the correct values for the magnetic vectorpotential at the left and right side of the finite element model. An equivalent magnetic reluctance is calculated out the stored magnetic energy *W*.

$$\Phi = \left(A_{left} - A_{right}\right) b \tag{14}$$

$$W = \frac{1}{2}\Re_m \Phi^2 \tag{15}$$

The same air gap is seen in two different ways, but with the same reluctance, to determine the correction factor k_f of the cross-section of the air gap.

$$\frac{k_c\, g}{\mu_0\, \lambda\, b} = \frac{g}{\mu_0\left(\lambda - w + 2\, k_f\, g\right) b} \tag{16}$$

$$k_f = \beta - \frac{\alpha}{2}. \tag{17}$$

The cross-section S_1 of the air gap beneath the centre leg of the E-core becomes (neglecting fringing in the third dimension)

$$S_1 = \left(a + 2\, k_f\, g\right) b. \tag{18}$$

Table 4 shows the result based on the Carter factor.

Fringing effect based on a Carter-like factor

The second factor is based on the Carter factor and can only be calculated using the finite element method. Instead of applying the Dirichlet boundary condition at the left hand side of the model, it is applied at the top side (fig. 5c).

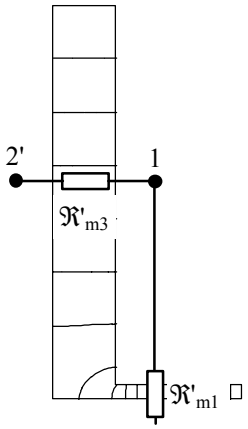

Figure 6: Approximation of the fringing effect using the Carter based factor.

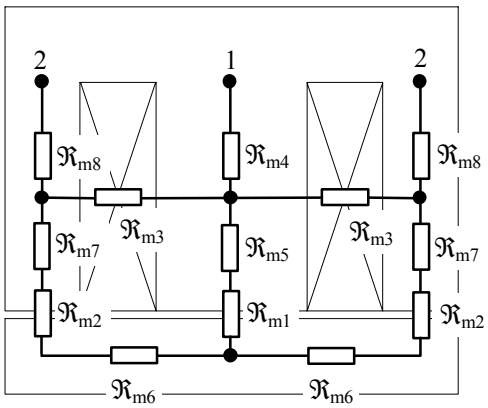

Figure 7: Magnetic circuit of the inductor with inclusion of the *MMF* drop in the iron.

Table 4: Inductance calculation with a better approximation of the fringing effect based on the Carter factor.

$k_c = 1.27$	k_c (FEM) = 1.28
$k_f = 1.61$	with
$\Re_{m1} = 4.133 \cdot 10^5$ H^{-1}	$W = 3.357 \cdot 10^3$ J
$\Re_{m2} = 7.187 \cdot 10^5$ H^{-1}	$\Phi = 0.09$ Wb
$\Re_{m3} = 8.842 \cdot 10^6$ H^{-1}	
$\Re_m = 6.579 \cdot 10^5$ H^{-1}	
$L = 0.126$ H	

Table 5: Inductance calculation with a better approximation of the fringing effect based on a Carter-like factor.

$W = 2.239 \cdot 10^3$ J	$\Re_{m2} = 8.111 \cdot 10^5$ H^{-1}
$\Phi = 0.09$ Wb	$\Re_{m3} = 8.842 \cdot 10^6$ H^{-1}
$k_f = 0.91$	$\Re_m = 7.114 \cdot 10^5$ H^{-1}
$\Re_{m1} = 4.423 \cdot 10^5$ H^{-1}	$L = 0.117$ H

Table 6: Inductance calculation with inclusion of the *MMF* drop in the iron parts.

$k_f = 0.91$	$\Re_{m5} = 6.837 \cdot 10^3$ H^{-1}
$\mu_r = 970$	$\Re_{m6} = 2.735 \cdot 10^4$ H^{-1}
$\Re_{m1} = 4.423 \cdot 10^5$ H^{-1}	$\Re_{m7} = 1.367 \cdot 10^4$ H^{-1}
$\Re_{m2} = 8.111 \cdot 10^5$ H^{-1}	$\Re_{m8} = 3.646 \cdot 10^4$ H^{-1}
$\Re_{m3} = 8.842 \cdot 10^6$ H^{-1}	$\Re_m = 7.579 \cdot 10^5$ H^{-1}
$\Re_{m4} = 9.115 \cdot 10^3$ H^{-1}	$L = 0.109$ H

The equivalent magnetic reluctance can be seen as a parallel connection (fig. 7) of the reluctance $\Re'_{m1}$ of the air gap, fringing included, and the reluctance $\Re'_{m3}$ of a rectangular slot with uniform field distribution. The value of $\Re'_{m1}$ is used to obtain the reluctance of the air gap with a better approximation of the fringing effect. Table 5 shows the result based on the Carter-like factor.

Inclusion of the magnetomotive force drop in the iron parts

Figure 8 shows a possible magnetic circuit including the magnetomotive force drop of the iron parts. The iron is assumed to be linear. Further refinement of this model is not necessary because a rough finite element model takes over. The average length of a flux line in each iron part is determined, to calculate the reluctance of that part. Table 6 gives the results of this calculation. The knowledge of the Y-Δ transformation is needed to simplify the magnetic circuit.

Inclusion of the non-linear behaviour of the iron parts results in flux dependent reluctances. The inductance can be obtained by solving a non-linear system of equations.

Superposition of flux-*MMF* plots

Another approach including the non-linear behaviour of the iron parts but not the leakage flux, is the superposition of the flux-*MMF* plot of the air gaps with the flux-*MMF* plots of the iron parts. Table 7 shows the working scheme. Due to the difference in magnetic flux through the left or right leg and the middle leg, both paths are seperately handled. The relation between the fluxes defines how the flux-*MMF* plots have to be combined. The flux-*MMF* plot of an air gap is defined by its reluctance. The flux-*MMF* plot of an iron part is obtained starting from the magnetization curve (fig. 8). Figure 9 shows the flux-*MMF* plots. The last step results in the inductance versus the current (fig. 10). Table 8 gives the value of the inductance for the rated value of the current.

FINITE ELEMENT APPROACH

The calculation of the inductance is based on the identification of the magnetic energy W stored in the inductor expressed in magnetic quantities

$$W = \int \left(\int H \, \mathrm{d}\, B \right) \mathrm{d}\, V \,, \tag{18}$$

and the same energy expressed in electric quantities

$$W = \frac{1}{2} L \, I^2 \,. \tag{19}$$

Figure 11 shows the flux plot of the finite element solution of the inductor, while table 9 shows the result of the finite element calculation of the inductance.

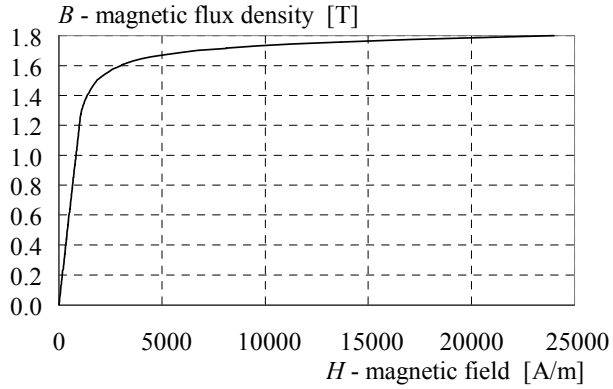

Figure 8: Non-linear magnetization curve of the iron parts.

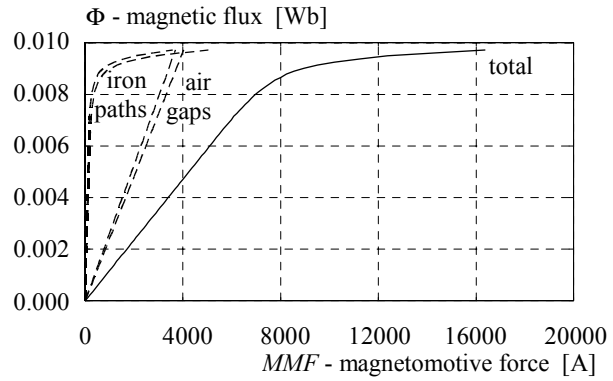

Figure 9: Total and partial flux-*MMF* plots.

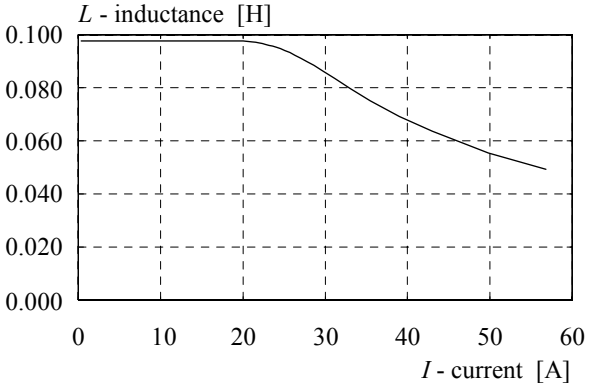

Figure 10: Calculation of the inductance by superposing the flux-*MMF* plots.

Table 7: Working scheme for the superposing of flux-*MMF* plots.

Step 1	H	$\Rightarrow$	B
Step 2	$MMF = H\,\ell$	$\Rightarrow$	$\Phi = B\,S$
Step 3	MMF	$\Rightarrow$	$\Phi = \dfrac{MMF}{\Re_m}$
Step 4	MMF	$\Rightarrow$	Φ
Step 5	$I = \dfrac{MMF}{N}$	$\Rightarrow$	$L = \dfrac{N\,\Phi}{I}$

Table 8: Calculation of the inductance by superposing the flux-*MMF* plots.

L = 0.097 H

CONCLUSION

The understanding of a simple magnetic system such as an inductor forms the basis of more difficult magnetic systems as electrical motors and gives an idea on what can be neglected during a finite element calculation. Comparing the different results shows the importance of fringing, leakage, *MMF* drop and non-linear behaviour. When a device can not be considered as infinity long as the E-core inductor, and a three dimensional finite element calculation is required, becomes also clear.

ACKNOWLEDGEMENT

The authors are grateful to the Belgian Nationaal Fonds voor Wetenschappelijk Onderzoek for its financial support of this work and the Belgian Ministry of Scientific Research for granting the IUAP No. 51 on Magnetic Fields.

REFERENCES

1. Binns, K. J., Lawrenson, P. J. and Trowbridge, C. W., *The Analytical and Numerical Solutions of Electric and Magnetic Fields*, John Wiley & Sons (1992).
2. Lowther, D. A. and Silvester, P. P., *Computer-Aided Design in Magnetics*, Springer-Verlag (1986).
3. Silvester, P. P. and Ferrari, R. L., *Finite elements for Electrical Engineers*, Cambridge University Press (1990).
4. de Jong, H. C. J., Lipo, T. A., Novtny, D. and Richter, E., *AC Machine Design*, University of Wisconsin-Madison, College of Engineering, August 23-25 (1993).
5. Carter, F. W., A Note on Airgap and Interpolar Induction, *JIEE* 29, 925 (1900).
6. Carter, F. W., The Magnetic Field of the Dynamo-Electric Machine, *JIEE* 64, 100 (1926).

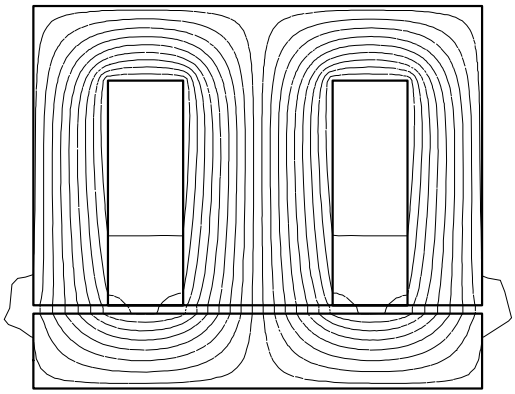

Figure 11: Flux plot of the inductor.

Table 9: Two dimensional finite element calculation of the inductance.

$W = 5.94$ J	$L = 0.119$ H